Progress In Electromagnetics Research, PIER 102, 107–124, 2010

APPLICATION OF STUB LOADED FOLDED STEPPED IMPEDANCE RESONATORS TO DUAL BAND FILTER DESIGN

M. D. C. Velázquez-Ahumada

Department of Electronics and Electromagnetism
University of Seville
Av. Reina Mercedes s/n, Seville 41012, Spain

J. Martel

Department of Applied Physics 2
University of Seville
Av. Reina Mercedes s/n, Seville 41012, Spain

F. Medina

Department of Electronics and Electromagnetism
University of Seville
Av. Reina Mercedes s/n, Seville 41012, Spain

F. Mesa

Department of Applied Physics 1
University of Seville
Av. Reina Mercedes s/n, Seville 41012, Spain

Abstract—In this paper, a folded stepped impedance resonator (SIR), modified by adding an inner quasi-lumped SIR stub, is used as a basis block for a new implementation of dual-band bandpass filters. The main advantage of the proposed filter is to make it possible to independently control the electrical features of the first and second bands. The behavior of the first band basically depends on the geometry of the outer folded SIR. The second band, however, is strongly influenced by the presence of the inner stub. Additional design flexibility is achieved by allowing the inner stub to be located at an arbitrary position along the high impedance line section of the main SIR. The position of the tapped input and output lines can be

Corresponding author: M. D. C. Velázquez-Ahumada (velazquez@us.es).

optimized in order to reach a reasonable matching of the filter at the central frequencies of both passbands. Some designs are reported to illustrate the possibilities of the proposed structure. Experimental verification has been included.

1. INTRODUCTION

Modern dual-band operation electronic devices require the development of efficient and compact dual-band filters. Indeed, the development of dual-band and multi-band filters is a very active research field nowadays [1–9]. Since microstrip implementation of dual-band filters is preferable for many applications, most of the cited papers deal with that technology. A variety of design techniques have been proposed in the literature to implement dual-band filters, and most of which can be accomplished in printed circuit technology. The composition of two simple band pass filters [10], the cascade connection of a large bandwidth bandpass filter with a stop-band filter [7, 11], filters built making use of two different types of resonators [12], filters incorporating defected ground structures [4], or filters based on the use of stepped-impedance resonators [9] are just a few examples of very different strategies followed by a number of researchers. The main disadvantage of some of the cited design methods is that they yield large size filters compared with implementations based on the use of small, intrinsically dual-band, resonators. In order to reduce the overall size of dual-band filters, a design based on the use of a double-layered substrate was proposed in [8]. Even so, nowadays, the trend is the design of filters whose individual components have a double bandpass response *per se* (see, for instance, [13]). Some of the filters of this class that have been studied during the last few years are made up of lines loaded with stubs [9, 14–16] (distributed circuit operation). More compact layouts are based on coupled resonators (of different types) designed in such a way that the two first resonance frequencies of the resonators coincide with the central frequencies of the two passbands [17–21].

Following the general rationale based on the use of intrinsically dual-band resonators, the authors have recently proposed a new compact resonator whose resonance frequencies can be separately selected [22]. The symmetrical version of such resonator was simultaneously proposed by J.-S. Hong [23]. This resonator is a modified version of the conventional folded stepped impedance resonator, or slow-wave resonator, described, for instance, in [24, chap. 11]. The modification consists in the introduction of a quasi-lumped SIR-type stub at the center of the high characteristic impedance section

of the original folded SIR. A drawing of such resonator can be seen in Fig. 1(a). In this structure, the first resonance frequency only depends on the dimensions of the external folded SIR, whereas the second resonance frequency is determined by both the external SIR and the quasi-lumped SIR-like stub. This fact allows for the independent tuning of the two operation frequencies. This is in contrast with what happens with conventional SIR's, where any change of their dimensions has an important impact on both frequencies. A similar concept has recently been applied in a couple of papers [25, 26] but, in those cases, open loop resonators loaded with open end microsinternaltrip stubs were used. The difference with our proposal lies on the fact that open loops work under $\lambda/2$ operation. This causes the size of the designs to be appreciably larger than those based on our new alternative. Since the size of folded SIR's is much smaller than that of open loops, the tuning element has to be chosen small enough due to space restrictions. For this reason, the tuning stub in our design is also a miniaturized SIR element, which provides the required reactance with smaller size than simple uniform stubs.

The present paper extends our previous work in [22] and provides more details of the working principle of the proposed resonators and about the design methodology. In particular, the influence of the substrate thickness on the coupling level between resonators is studied, as well as the possibility of designing higher order filters. It will be shown that filters based on coupled symmetric resonators allow fine tuning of the central frequencies of the two passbands, but once the bandwidth of one of the bands is established, the bandwidth of the other band is fixed. However, asymmetric versions of the stub loaded folded SIR are shown to provide control on the features of the second passband. The working principle is explained in detail and the method is used to design three different filters using symmetric and asymmetric pairs of resonators and a three resonators implementation of a higher order filter. Simulated and measured results agree reasonably well and are close to the behavior predicted by the original prototype.

2. CHARACTERIZATION OF THE RESONATORS

2.1. Symmetrical Structure

The layout of a modified symmetrical folded SIR, with a quasi-lumped stub connected to the central position of the high impedance line, is shown in Fig. 1(a). This configuration can be analyzed in terms of even and odd excitations (the AA' plane behaves as an electric/magnetic wall for odd/even excitation). For odd excitation, the centered tuning stub has no influence on the electrical response. This can be seen from

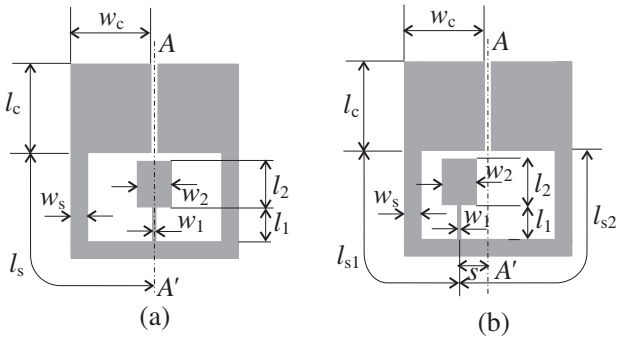

Figure 1. (a) Symmetric and (b) asymmetric modified folded SIR's used as basic resonators in this paper (figure from [22]).

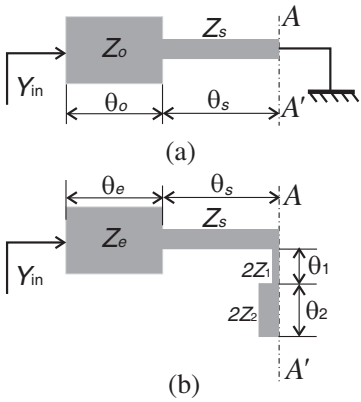

Figure 2. Approximate transmission line circuit model of the symmetrical SIR in Fig. 1(a) Odd excitation; (b) Even excitation (figure from [22]).

its equivalent circuit shown in Fig. 2(a) [25]. However, this stub is relevant under even excitation conditions. The equivalent circuit in Fig. 2(b) obviously accounts for its presence. Referring to Fig. 1(a), Z_s and θ_s denote the impedance and electrical length of the high impedance microstrip line section of the main folded SIR (length l_s and width w_s). $Z_{o,e}$ and $\theta_{o,e}$ are the modal (odd and even) impedances and electrical lengths of the two low impedance coupled lines appearing in the folded SIR (length l_c and width w_c). Finally, Z_i and θ_i are the characteristic impedances and electrical lengths of the sections of length l_i and width w_i $(i = 1, 2)$ of the inner SIR stub. The separation

between the low impedance coupled lines in the SIR has been kept equal to the minimum achievable slot width (≈ 100 μm for the fabrication process used in our laboratory). The following resonance frequencies for the odd and even excitations can be separately extracted from condition $Y_{\text{in}} = 0$:

a) Odd excitation resonance condition:

$$\tan\theta_s \tan\theta_o = R_o \tag{1}$$

b) Even excitation resonance condition:

$$\frac{1}{2R_1}\left[1 + \frac{\tan\theta_e \tan\theta_1}{R_e}\right]\left[\frac{\tan\theta_1}{R_1} + \frac{\tan\theta_2}{R_2}\right] + \left[\tan\theta_s + \frac{\tan\theta_e}{R_e}\right]\left[\frac{1}{R_1} + \frac{\tan\theta_1 \tan\theta_2}{R_2}\right] = 0 \tag{2}$$

where it has been introduced the dimensionless ratios $R_{o,e} = Z_{o,e}/Z_s$ and $R_i = Z_i/Z_s$ $(i = 1, 2)$.

As expected from Fig. 2 and Eqs. (1) and (2), the resonance frequencies for odd excitations exclusively depend on the outer folded SIR geometry, whereas those of even excitations depend on both, the external SIR and the inner stub. This fact makes it possible to design dual-band filters with independent control of the passband central frequencies. Thus, the first band (associated with the first odd resonance) is adjusted by varying the dimensions of the external resonator. Once this frequency has been obtained, the central frequency of the second band (corresponding to the first even resonance) can be tuned by a proper choice of the dimensions of the inner stub. This adjustment does not affect the frequency of the first resonance. As an example, we have obtained the four first resonances of a symmetrical resonator such as that shown in Fig. 1(a). In Fig. 3, these frequencies have been plotted as a function of the width w_2 using l_2 as parameter, while the total length of the tuning stub (l_1+l_2) is kept constant. We have distinguished between those resonance frequencies corresponding to odd excitation, f_1^o and f_2^o (they do not depend on the stub dimensions), and those corresponding to even excitation, f_1^e and f_2^e (they are sensitive to the presence of the stub). When designing the corresponding dual-band filter, from Fig. 3 we can extract the range of values within which it is possible to tune the central frequency of the second band (f_1^e). The third resonance frequency (f_2^o or f_2^e) gives information about the behavior of the filter beyond the second band. As mentioned above, we must vary the external SIR dimensions to tune the first resonance frequency, f_1^o. For instance, in Fig. 4, we show

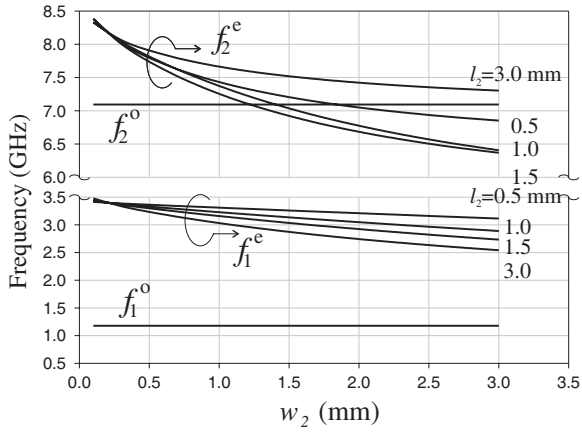

Figure 3. Behavior of the first four resonance frequencies of a symmetric resonator as a function of w_2 (l_2 is used as a parameter). Dimensions: $l_s = 8.35\,\text{mm}$, $w_s = 0.37\,\text{mm}$, $l_c = 4.3$ mm, $w_c = 4.3\,\text{mm}$, $w_1 = 0.2\,\text{mm}$, $l_1 + l_2 = 3\,\text{mm}$. The resonator is printed on a substrate with nominal permittivity $\varepsilon_r = 9.9$ and thickness $h = 0.635\,\text{mm}$ (data from [22]).

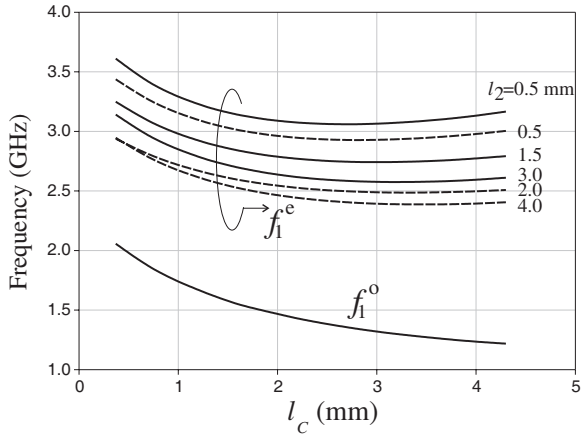

Figure 4. Behavior of the first two resonance frequencies of a symmetric resonator versus l_c ($l_c + l_s = 12.65\,\text{mm}$ in all cases, thus the physical size of the resonator is always the same). Dimensions: $w_s = 0.37\,\text{mm}$, $w_c = 4.3\,\text{mm}$, $w_1 = 0.2\,\text{mm}$, $w_2 = 3\,\text{mm}$, $l_1 + l_2 = 3\,\text{mm}$ (solid lines) and 4 mm (dashed lines). The resonator is printed on the same substrate used for data in Fig. 3.

the dependence of f_1^o on the length of the coupled lines, l_c, when the physical size of the resonator (the length $l_s + l_c$) remains invariable. As expected, the bigger the value of l_c, the smaller the value of f_1^o, since the resonator is electrically smaller and smaller. Similarly to Fig. 3, in Fig. 4, we have also included the values of the second resonance frequency, f_1^e, obtained for two stub lengths and different values of l_2.

2.2. Asymmetrical Structure

Higher design flexibility is achieved by allowing the stub to shift along the high impedance line section (see Fig. 1(b)). When this happens, the structure is no longer symmetrical and the analysis in terms of even/odd excitations cannot be applied. The analysis has now to be carried out by using the equivalent circuit in Fig. 5. This circuit can be seen as a parallel connection of the open-ended coupled lines (modal impedances Z_e and Z_o) and the T-circuit composed of two transmission lines of impedance Z_s and the open SIR stub (impedances Z_1 and Z_2). The resonance frequencies can be obtained following the rationale in [28], for instance. It will be shown later that the distance, s, between the middle of the inner stub and the axis AA' plays an essential role to determine the coupling between resonators at the second resonance. Our aim is to use s to control that coupling, for which it would be desirable that the two first resonance frequencies keep almost constant as s varies. This is approximately satisfied provided that the electrical length of the stub is small up to the second resonance frequency. The first four resonance frequencies of an example case have been tabulated in Table 1. Since the electrical length of the stub increases with frequency, the higher the resonance frequency order, the stronger its

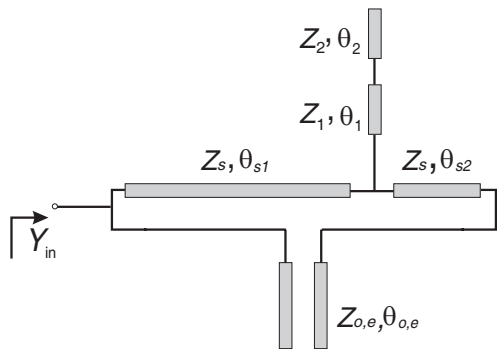

Figure 5. Transmission line model of the asymmetric resonator (figure from [22].

Table 1. Values of the four first resonance frequencies (in GHz) of an asymmetric resonator for different values of s. Referring to Fig. 1(b), $l_{s1} + s = 8.35$ mm, $w_0 = 0.37$ mm, $l_c = w_c = 4.3$ mm, $w_1 = 0.2$ mm, $l_1 = 0.6$ mm, $w_2 = 2.55$ mm, and $l_2 = 2.55$ mm. The substrate is the same as in Fig. 3.

s (mm)	f_1	f_2	f_3	f_4
0	1.218	2.686	6.742	7.053
0.5	1.217	2.691	6.556	7.257
1	1.216	2.704	6.314	7.591
1.5	1.214	2.727	6.073	7.965
2	1.212	2.760	5.850	8.369
2.5	1.209	2.804	5.644	8.782

Table 2. Values of the resonance frequencies of the structure (in GHz) of Table 1 after adjusting w_2.

s (mm)	w_2 (mm)	f_1	f_2	f_3	f_4
0	2.55	1.218	2.686	6.742	7.053
0.5	2.57	1.217	2.687	6.563	7.256
1	2.64	1.216	2.687	6.302	7.585
1.5	2.75	1.215	2.688	6.048	7.951
2	2.93	1.211	2.688	5.807	8.344
2.5	3.20	1.209	2.685	5.575	8.740

dependence with s. But for the first two resonances (electrically small stub), the dependence of f_1 with s is negligible whereas f_2 changes around 4%. In order to compensate for this change, the stub has been adjusted so that both the first and the second resonance frequencies remain the same for all the stub positions (we have slightly modified the value of w_2 for each value of s). After this process, the frequency values of Table 1 have been recalculated and shown in Table 2. It is worth emphasizing the practical importance of the asymmetric structure. Changing the position of the inner stud allows the designer to independently control the coupling level between adjacent resonators for each of the two passbands. Symmetric resonators allow independent tuning of the central frequencies, but once the bandwidth and ripple of the first band are specificied, the second band can not be tuned because coupling between resonators was optimized for the first band. The use of asymmetric resonators add flexibility because independent

tuning of coupling level for each band can be achieved. This makes it possible independent specification of the bandwidths for each of the passbands within a certain range of values. This will be experimentally shown in the forthcoming section.

3. DESIGN METHODOLOGY FOR FILTERS BASED ON MODIFIED SIR

3.1. Symmetric Configuration

The design methodology for dual-band filters based on the proposed resonators is close to the procedure in [24] for filters with a single passband and direct coupling. If the resonator of Fig. 1(a) is used, the first step is to adjust the dimensions of the external SIR so that its first resonance frequency is the central frequency of the first passband, f_1. Then, the inner stub must be designed so that the second resonance fits f_2 (i.e., the central frequency of the second band). The dimensions of the outer SIR and those of the inner stub have been obtained from the model in Fig. 2 (note that it is possible to choose among several geometries that have the same two first resonance frequencies, f_1 and f_2). The next step is to obtain the coupling coefficients, M_i at f_i $(i = 1, 2)$, from the specs of the first passband (fractional bandwidth, Δ_i, and ripple, r_{pi} $(i = 1, 2)$) as a function of the coupling distance, d. This task has been carried

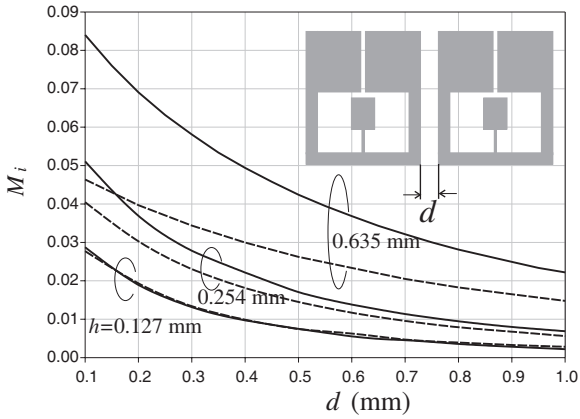

Figure 6. Coupling coefficients M_1 (dashed lines) and M_2 (solid lines) as functions of the distance between symmetrical resonators for different substrate thicknesses. Resonator dimensions are given in the main text.

out by using the commercial electromagnetic solver *Ensemble*. The coupling coefficients of a pair of symmetric resonators as a function of d are shown in Fig. 6 for three different substrate thicknesses, h (substrate permittivity: $\varepsilon_r = 9.9$). The dimensions of the resonator have been calculated in such a way that they have the same two first resonance frequencies: for $h = 0.635\,\text{mm}$, dimensions are the same as those in Fig. 3 ($w_2 = 2.55$ mm); for $h = 0.254\,\text{mm}$, we have obtained $w_s = 0.37\,\text{mm}$, $w_c = 3.57\,\text{mm}$, $l_s = 7.04\,\text{mm}$, $l_c = 4.3\,\text{mm}$, $w_1 = 0.2\,\text{mm}$, $w_2 = 2.42\,\text{mm}$, $l_1 = 0.5$ mm, and $l_2 = 2.12$ mm; and for $h = 0.127\,\text{mm}$, $w_s = 0.37\,\text{mm}$, $w_c = 3.01\,\text{mm}$, $l_s = 6.48\,\text{mm}$, $l_c = 4.3$ mm, $w_1 = 0.2\,\text{mm}$, $w_2 = 2.12\,\text{mm}$, $l_1 = 0.41$ mm and $l_2 = 2.12$ mm. As can be seen from Fig. 6, the coupling factors are strongly influenced by the substrate thickness, so this parameter can be conveniently used to achieve the required values of M_1 and M_2. Anyway, adjustment of both, the dimensions of the outer SIR and the inner stub (keeping the same values of f_1 and f_2), for each substrate thickness, it is another method to get values of M_1 and M_2 different from those extracted from Fig. 6. Note that, once the couplings have been chosen for the first band, the second band is determined. The bandwidth of this second band can not be tuned using the symmetric resonators.

3.2. Asymmetric Configuration

When using the asymmetric resonator in Fig. 1(b) to design a dual-band filter, the procedure is very similar to that described for the symmetric case, but with an interesting advantage. In Fig. 7, we have plotted the coupling coefficients M_1 and M_2 versus t (which stands for the position of the inner stub) using the distance between resonators, d, as parameter. It should be noted that, for each value of t, the inner stub has been adjusted in order to keep invariable the two first resonance frequencies of the resonator. The dimensions and substrate are the same as in the symmetric case ($h = 0.635$ mm). As it can be seen in Fig. 7, the coupling factor in the first band, M_1, does not meaningfully depend on the position of the stub, whereas the coupling factor of the second band, M_2, strongly depends on that position. In other words, by means of a simple stub shift, we can control the coupling factor of the second band *without modifying the coupling factor of the first band*. Therefore, without any change of the outer SIR dimensions, the range of the M_1 and M_2 values (and the possibilities for the fractional bandwidths Δ_1 and Δ_2) is much greater in the asymmetric configuration than in the symmetric one. Similar conclusions can be extracted from Fig. 8, where we have plotted the coupling factor between a symmetric resonator and an asymmetric one as a function of the position t of the inner stub, for different values of

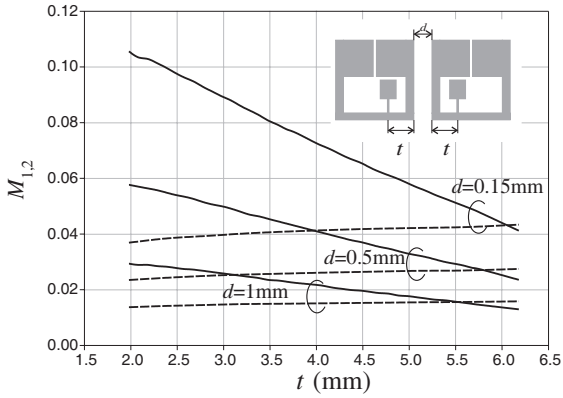

Figure 7. Coupling coefficients M_1 (dashed lines) and M_2 (solid lines) between two asymmetrical resonators, as a function of the internal shift of the stub (t) using the distance d as parameter.

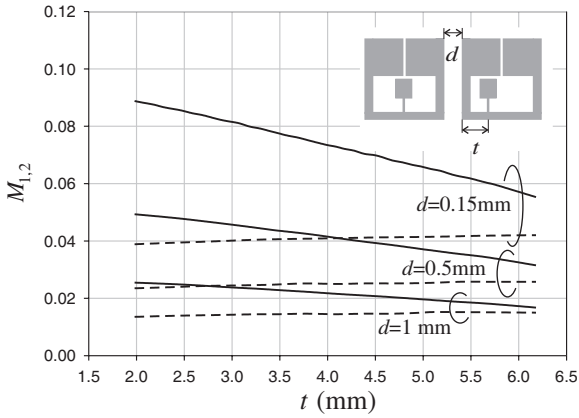

Figure 8. Coupling coefficients M_1 (dashed lines) and M_2 (solid lines) between a symmetrical resonator and an asymmetrical one as a function of the internal shift of the stub using the distance d as parameter.

the distance d. This coupling configuration is useful in the design of filters using an odd number of resonators. In such cases the central resonators must be symmetrical, while the surrounding resonators are asymmetrical. In all the examples, the last step of the design consists in matching the two passbands simultaneously. This goal can be achieved by following a procedure similar to that described in [18]. However, in order to avoid dual frequency transforms (which can enlarge the size

of the filter), we have employed the electromagnetic simulator to find the optimal dimensions and position of tapped lines. The position of the feeding lines has been modified looking for acceptable matching at the two passbands.

4. EXAMPLES OF DESIGN

In order to illustrate the previously introduced concepts, we have designed three dual-band filters with the bands centered at $f_1 = 1.21\,\text{GHz}$ and $f_2 = 2.65\,\text{GHz}$ using both symmetric and asymmetric resonators (central frequencies have been arbitrarily chosen; they do not correspond to any specific application). Photographies of the fabricated and measured filters are shown in Fig. 9. The dimensions of the resonators are exactly the same as those employed in the theoretical study. The specifications of filter (A) (based on the use of symmetric resonators) for the first band are: order $N = 2$, ripple, $r_{p1} = 0.1\,\text{dB}$, $\Delta_1 = 3.3\%$. From these values, using the curves in Fig. 6, we extract the distance $d = 0.15$ mm. This value enforces the second band specifications to be: $r_{p2} = 0.15\,\text{dB}$ and $\Delta_2 = 10\%$. The simulated and measured responses of filter (A) are shown in Fig. 10. The agreement between simulation and measurement is quite good in the whole explored frequency band. It is important to emphasize that, in the optimization process of the dimensions and position of the tapped lines, we achieve a transmission zero between the two passbands. This fact improves the filter selectivity. Fig. 10 includes details of the two passbands.

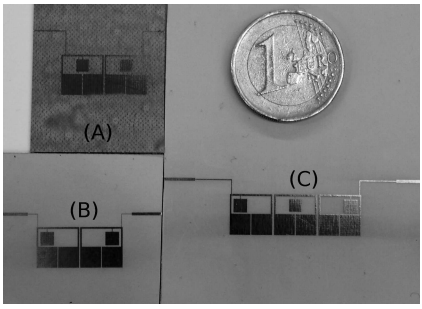

Figure 9. Photographs of the fabricated and measured filters: (A) filter based on two identical symmetric resonators; (B) filter based on two coupled asymmetric resonators allowing independent tuning of the second pass band; (C) higher order filter using two asymmetric resonators and one central symmetric resonator.

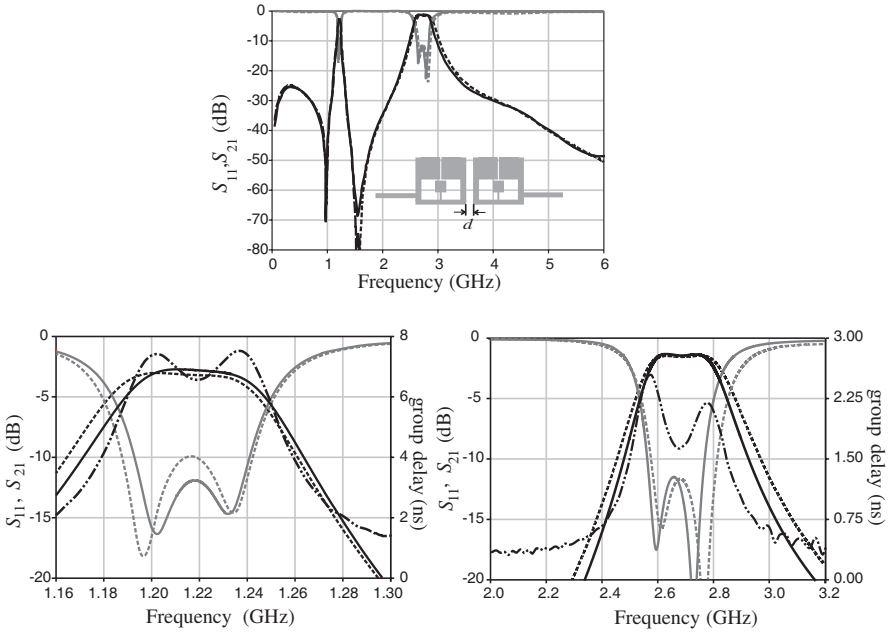

Figure 10. Simulated (dashed lines) and measured (solid lines) response of filter A designed using symmetrical resonators. Grey lines correspond to S_{11} and black lines correspond to S_{12}. Bottom figures show details of the two passbands (including group delay; dots correspond to group delay.

In the case of filter (B), with order $N = 2$, the asymmetric version of the resonators is used. This allows us to establish the specs of the two passbands: for the first band, $r_{p1} = 0.1\,\text{dB}$ and $\Delta_1 = 3.5\%$; for the second band, $r_{p2} = 0.1\,\text{dB}$ and $\Delta_2 = 4\%$. For these values, we can obtain, from Fig. 7, the distances $d = 0.15\,\text{mm}$ and $t = 6.45$ mm. In Fig. 11 the simulated and measured responses of the designed filter are shown. Again, a reasonable agreement has been found between both results. Note that, in this case, the specs of the second band have been independently established. In the previos example, filter (A), the bandwidth of the second band was fixed once the first band had been specified. It is worth mentioning that the high frequency behavior of the filters (A) and (B) in the out of band region is quite different because asymmetruc resonators have more resonance frequencies than the symmetric ones. The designer must be careful with higher order resonances.

Finally, let us design a higher order filter to demonstrate the possibility of applying the new resonators to dual band filters of

superior order. In particular, we have implemented a filter of order $N = 3$, filter (C) in Fig. 9, with the following specs: for the first band, Butterworth response ($r_{p1} = 0$) and $\Delta_1 = 4.3\%$; for the second band, $r_{p2} = 0.1$ dB and $\Delta_2 = 6\%$. In such a filter, direct couplings are between the central symmetrical resonator and the asymmetrical ones at the input and output ports. Thus we have used the curves in Fig. 8 to extract the distances $t = 6.65\,\text{mm}$ and $d = 0.33\,\text{mm}$ for the specs values. Measured and simulated filter responses are provided in Fig. 12. As in the previous designs, the agreement between measured and simulated results is reasonably good (discrepancies are attributed to dimensional tolerances). It should be noted that the out-of-band rejection level of the third order implementation is much better than that of the second order one (in particular in the low end of the spectrum). As expected, losses in the passbands are worse than in the case of lower order filters. However, the out-of-band rejection level is much better in the high order filter.

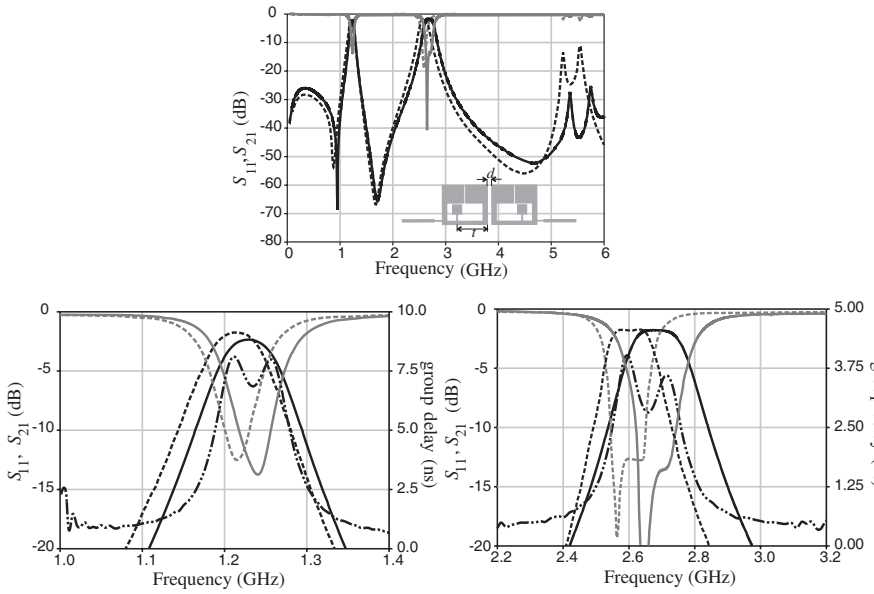

Figure 11. Simulated (dashed lines) and measured (solid lines) response of filter B designed using asymmetrical resonators. Grey lines correspond to S_{11} and black lines correspond to S_{12}. Bottom figures show the two passbands details, including group delay. Dots correspond to group delay.

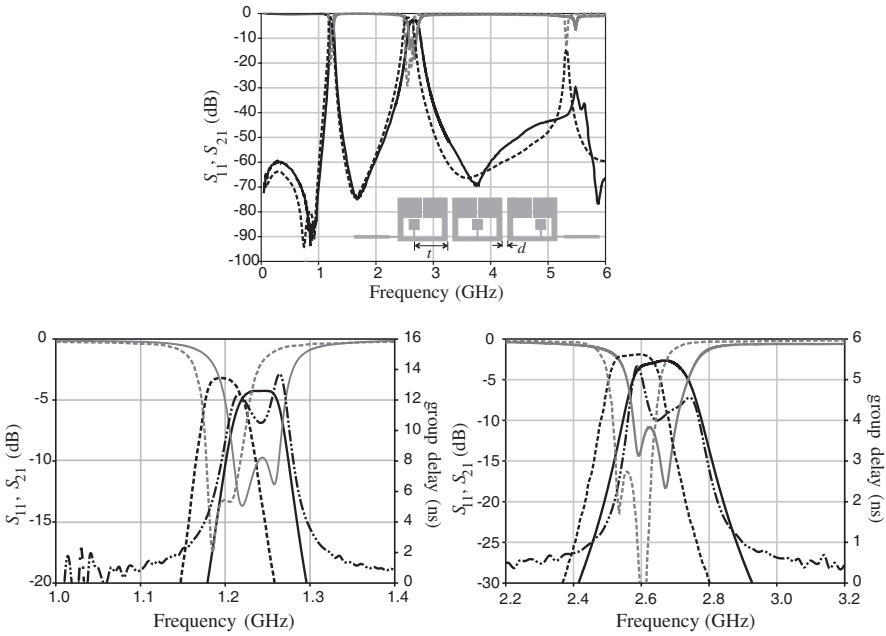

Figure 12. Simulated (dashed lines) and measured (solid lines) response of filter C designed on the basis of the combination of symmetrical and asymmetrical resonators. Grey lines correspond to S_{11} and black lines correspond to S_{12}. Bottom figures show the two passbands details, including group delay. Dots correspond to group delay.

5. CONCLUSION

This paper has presented a new planar and compact resonator based on a simple modification of the conventional folded SIR. The modification consists in adding an inner SIR type stub connected to the high impedance line of the main resonator. The possibility of using symmetric and asymmetric versions of the new resonators to design dual-band filters has been investigated. We have found that, in the case of the asymmetric resonator, the filter design is much more flexible because we can separately design the specifications of the two bands without modifying the geometry of the external SIR: the fractional bandwidth of the first band can be controlled by means of the distance between resonators and the fractional bandwidth of the second band by means of the inner stub position. Three filters have been designed, built and measured, finding in all designs good agreement between simulated and measured filter responses.

ACKNOWLEDGMENT

This work has been funded by the Spanish Ministerio de Ciencia e Innovación (project no. TEC2007-65376) and by the Spanish Junta de Andaluca (project TIC-4595 and grant TIC-112).

REFERENCES

1. He, Z. N., X. L. Wang, S. H. Han, T. Lin, and Z. Liu, "The synthesis and design for new classic dual-band waveguide band-stop filters," *Journal of Electromagnetic Waves and Applications*, Vol. 22, No. 1, 119–130, 2008.
2. Dai, X.-W., C.-H. Liang, B. Wu, and J.-W. Fan, "Novel dual-band bandpass filter design using microstrip open-loop resonators," *Journal of Electromagnetic Waves and Applications*, Vol. 22, No. 2/3, 219–225, 2008.
3. Li, G., B. Wu, X.-W. Dai, and C.-H. Liang, "Design techniques for asymmetric dual-passband filters," *Journal of Electromagnetic Waves and Applications*, Vol. 22, No. 2/3, 375–383, 2008.
4. Wang, J. P., B. Z. Wang, Y. X. Wang, and Y. X. Guo, "Dual-band microstrip stepped-impedance bandpass filter with defected ground structure," *Journal of Electromagnetic Waves and Applications*, Vol. 22, No. 4, 463–470, 2008.
5. Dai, X.-W., C.-H. Liang, G. Li, and Z.-X. Chen, "Novel dual-mode dual-band bandpass filter using microstrip meander-loop resonators," *Journal of Electromagnetic Waves and Applications*, Vol. 22, No. 4, 573–580, 2008.
6. Hsu, C.-Y., H.-R. Chuang, and C.-Y. Chen, "Compact microstrip UWB dual-band bandpass with tunable rejection band," *Journal of Electromagnetic Waves and Applications*, Vol. 23, No. 5/6, 617–626, 2009.
7. Abu-Hudrouss, A. M. and M. J. Lancaster, "Design of multiple-band microwave filters using cascaded filter elements," *Journal of Electromagnetic Waves and Applications*, Vol. 23, No. 10, 2109–2118, 2009.
8. Weng, R. M. and P. Y. Hsiao, "Double-layered quad-band bandpass filter for multi-band wireless systems," *Journal of Electromagnetic Waves and Applications*, Vol. 23, No. 3, 2153–2161, No. 16, 2009.
9. Alkanhal, M. A. S., "Dual-band bandpass filters using inverted stepped-impedance resonators," *Journal of Electromagnetic Waves and Applications*, Vol. 23, No. 8/9, 1211–1220, 2009.

10. Myyake, H., S. Kitazawa, T. Ishizaki, T. Yamada, and Y. Nagatomi, "A miniaturized monolithic dual band filter using ceramic lamination technique for dual mode portable telephones," *IEEE-MTT-S International Microw. Symp. Dig*, Vol. 2, 789–792, 1997.
11. Tsai, L. C. and C. W. Huse, "Dual-band bandpass filters using equal length coupled-serial-shunted lines and Z-transform techniques," *IEEE Trans. on Microwave Theory and Tech.*, Vol. 52, No. 4, 1111–1117, Apr. 2004.
12. Chen, C. Y. and C. Y. Hsu, "A simple and effective method for microstrip dual band design," *IEEE Microw. Wireless Compon. Lett.*, Vol. 16, No. 3, 246–258, May 2006.
13. García-Lampérez, A. and M. Salazar-Palma, "Dual band filter with split-ring resonators," *IEEE MTT-S International Microw. Symp. Dig.*, 519–522, 2006.
14. Quendo, C., E. Rius, and C. Person, "An original topology of dual-band filter with transmission zeros," *IEEE-MTT-S International Microw. Symp. Dig.*, Vol. 2, 1093–1096, 2003.
15. Tsai, C. M., H. M. Lee, and C. C. Tsai, "Planar filter design with fully controllable second passband," *IEEE Trans. on Microwave Theory and Tech.*, Vol. 53, No. 11, 3429–3439, Nov. 2005.
16. Chin, K. S., J. H. Yeh, and S. H. Chao, "Compact dual-Band bandstop filters using stepped-impedance resonators," *IEEE Microw. Wireless Compon. Lett.*, Vol. 17, No. 12, 849–851, Dec. 2007.
17. Kuo, J. T. and H. S. Cheng, "Design of quasi-elliptic function filters with a dual-passband response," *IEEE Microw. Wireless Compon. Lett.*, Vol. 14, No. 10, 472–475, Oct. 2004.
18. Kuo, J. T., T. H. Yeh, and C. C. Yeh, "Design of microstrip bandpass filters with a dual-passband responds," *IEEE Trans. on Microwave Theory and Tech.*, Vol. 53, No. 4, 1331–1337, Apr. 2005.
19. Sun, S. and L. Zhu, "Compact dualband microstrip bandpass filter without external feed," *IEEE Microw. Wireless Compon. Lett.*, Vol. 15, No. 10, 644–646, Oct. 2005.
20. Zhang, Y. P. and M. Sun, "Dual-band microstrip passband filter using stepped-impedance resonators with new coupling scheme," *IEEE Trans. on Microwave Theory and Tech.*, Vol. 54, No. 10, 3779–3785, Oct. 2006.
21. Weng, M. H., H. W. Wu, and Y. K. Su, "Compact and low loss dual-band bandpass filter using pseudo-interdigital stepped

impedance resonators for WLANs," *IEEE Microw. Wireless Compon. Lett.*, Vol. 17, No. 3, 187–189, Mar. 2007.

22. Velázquez-Ahumada, M. C., J. Martel, F. Medina, and F. Mesa, "Design of a dual band-pass filter using modified folded stepped-impedance resonators," *IEEE-MTT-S International Microw. Symp. Dig.*, 857–860, 2009.
23. Hong, J.-S. and W. Tang, "Dual-band filter based on non-degenerate dual-mode slow-wave open-loop resonators," *IEEE-MTT-S International Microw. Symp. Dig.*, 861–864, 2009.
24. Hong, J. S. and M. J. Lancaster, *Microstrip Filters for RF/Microwave Applications*, Wiley Inter-Science, New York, 2001.
25. Zhang, X. Y., J.-X. Chen, Q. Xue, and S. M. Li, "Dual-band bandpass filters using stub-loaded resonators," *IEEE Microw. Wireless Compon. Lett.*, Vol. 17, No. 8, 583–585, Aug. 2007.
26. Mondal, P. and M. K. Mandal, "Design of dual-band passband filters using stub-loaded open-loop resonators," *IEEE Trans. on Microwave Theory and Tech.*, Vol. 56, No. 1, 150–155, Jan. 2008.
27. Sagawa, M., M. Makimoto, and S. Yamashita, "Geometrical structures and fundamental characteristics of microwave stepped-impedance resonators," *IEEE Trans. on Microwave Theory and Tech.*, Vol. 45, No. 7, 1078–1085, Jul. 1997.
28. Makimoto, M. and S. Yamashita, *Microwave Resonators and Filters for Wireless Communications*, Springer Series in Advanced Microelectronics, Berlin, 2001.